Science of the Total Environment 640–641 (2018) 570–580

Contents lists available at ScienceDirect

Science of the Total Environment

journal homepage: www.elsevier.com/locate/scitotenv

Marginal-cost-based greedy strategy (MCGS): Fast and reliable optimization of low impact development (LID) layout

Te Xu [a], Bernard A. Engel [b], Xinmei Shi [a], Linyuan Leng [a], Haifeng Jia [a,*], Shaw L. Yu [c], Yaoze Liu [b]

[a] School of Environment, Tsinghua University, Beijing, China
[b] Department of Agricultural & Biological Engineering, Purdue University, West Lafayette, IN, USA
[c] Department of Civil & Environmental Engineering, University of Virginia, Charlottesville, VA, USA

HIGHLIGHTS

- A fast and reliable method, MCGS, is developed for LID layout optimization.
- MCGS is based on the law of increasing marginal costs and rational choice theory.
- Three case studies with different settings prove broad applicability of MCGS.
- MCGS is superior to NSGA-II in five prominent advantages.
- MCGS addresses concerns of multi-stage LID layout planning.

GRAPHICAL ABSTRACT

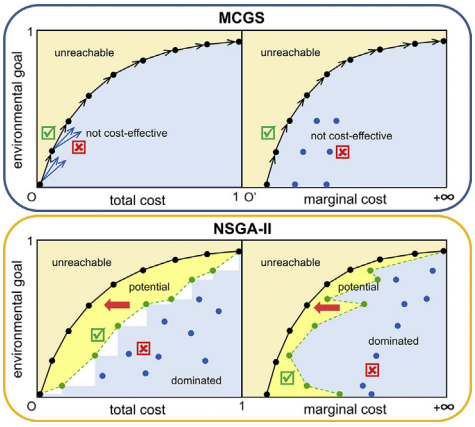

ARTICLE INFO

Article history:
Received 13 April 2018
Received in revised form 28 May 2018
Accepted 28 May 2018
Available online 2 June 2018

Editor: Frederic Coulon

Keywords:
Stormwater management
Low impact development
Optimization
Marginal cost
Greedy strategy
NSGA-II

ABSTRACT

Cost effectiveness is a major concern when implementing low impact development (LID) practices for urban stormwater management (USWM). To optimize LID layout, an efficient and more reliable method, namely, the Marginal-Cost-based Greedy Strategy (MCGS) was developed based on the economic law of increasing marginal costs (MCs) and the stepwise minimization of MCs. To verify its broad applicability, MCGS was applied in three case studies in China with different system settings and environmental goals. Both Cases I and II were watershed-scale studies in Suzhou City urban districts, but in Case II, the impact of future uncertainties (i.e., climate change, urban expansion, and LID performance degradation) on USWM system performance was considered. Case III was a block-scale study of the Xixian New District (a pilot "Sponge City" in China), which involved a rainwater pipe network and a complicated environmental goal. Compared with the extensively used but complicated NSGA-II, the MCGS performed better in terms of yielding more converged performance trade-offs, providing more choices for city planners, and requiring much less computational resources in all three cases. Meanwhile, MCGS established an optimal pathway for multi-stage LID layout planning. The success of MCGS indicated that the MC of a LID practice determined its favorability in an USWM system.

* Corresponding author.
E-mail address: jhf@tsinghua.edu.cn (H. Jia).

https://doi.org/10.1016/j.scitotenv.2018.05.358
0048-9697/

1. Introduction

Recent decades witness a rapid urbanization worldwide. In China, for example, its urban population has grown to 52.4% in 2015 from 42.5% in 2005, and the build-up areas have increased by 17,252 km^2 over the past decade (Jia et al., *2017*). Rapid urbanization has caused severe a "city syndrome," including urban flooding, non-point source (NPS) pollution, water shortage, and landscape and ecological degradation, which is threatening public health (Larsen et al., *2016*; Versini et al., *2018*). This situation is worsening with continuing population growth and economic development, rapidly growing impervious ratios in urban areas, frequent occurrence of extreme weather conditions, and an increased resident demand for amenity and access to urban landscape (Ferguson et al., *2013*; Urich and Rauch, *2014*; He et al., *2015*; Wang et al., *2017*). Therefore, urban stormwater management (USWM) has become a significant action item for city planners and government leaders.

The worldwide recognized concept of low impact development (LID), i.e., decentralized measures (e.g., green roof, porous pavement, and bioretention), which treat in-situ stormwater runoff along the flow path (Prince George's County, *1999*; USEPA, *2008*), are proven effective and environmentally friendly for USWM (e.g., urban flooding control, peak flow reduction, NPS pollution removal, and rainwater utilization) (Clausen and Bedan, *2009*; Fletcher et al., *2014*; Askarizadeh et al. *2015*; Liu et al., *2015a*). LID practices also provide multifunctional (e.g., environmental, ecological, and socio-economic) services and strengthen urban resilience to deal with the uncertainties of future developments (Marlow et al., *2013*; Meerow and Newell, *2017*; Wang et al., *2018*). Inspired by this eco-environmentally sound concept, a national program, namely, "Sponge Cities" has been initiated in China since 2013, targeting at solving or alleviating the "city syndrome" (Gaines, *2016*). Annually, this program is devoting an enormous amount of resources to pilot cities for LID practice planning/implementation for stormwater runoff control, as an indispensable component to the grey infrastructure that has typically been used in USWM (Jia et al., *2017*). How to select proper LID practices, determine their suitable size, and place them in right locations are essential when drafting LID layout schemes within the constraint of the given investment. The officials and the public are all concerned about getting a positive multifunctional return, especially for the environmental aspects. A balance between competing environmental and economic concerns is urgently required (Xu et al., *2017*). Previous studies (Bark et al. *2015*; Cano and Barkdoll *2017*; Liu et al., *2016a*) have indicated that a multi-objective LID layout optimization can address these concerns.

Multi-objective evolution algorithm (MOEA) is a powerful tool with general applicability for solving multi-objective problems (MOPs) with several contradictory objectives. Oraei Zare et al. (*2012*) and Xu et al. (*2017*) successfully achieved a trade-off between the environmental and economic indicators by coupling the Non-Sorting Genetic Algorithm (NSGA-II) with the Storm Water Management Model (SWMM). NSGA-II was also a built-in module in the System for Urban Stormwater Treatment and Analysis IntegratioN (SUSTAIN) (Shoemaker et al., *2009*), which is useful for city planners to seek for a cost-effective planning scheme (Lee et al., *2012*; Jia et al., *2015*). However, its expensive computational cost and premature convergence are significant concerns, particularly when the system complexity increases dramatically, such as when multiple sites and LID practices need to be considered in a large planning area (Liu et al., *2016a*) or when future uncertainties, such as climate change and urban development, need to be considered (Urich and Rauch, *2014*; Liu et al., *2016b*). To address "the curse of dimensionality" of decision variables, Liu et al. (*2016a*) applied a dynamic planning strategy, that is, multi-level spatial optimization to conduct LID layout optimization in a watershed-scale area. However, this strategy largely relies on the hypothesis of independent hydrologic response units (HRUs) (Cibin and Chaubey *2015*), which may not be true in many real cases. In addition, a MOEA is a "black-box" approach. The underlying mechanism of selection and placement of suitable LID practices is too complicated and unclear for city planners to understand (Cano and Barkdoll *2017*) thereby lowering their confidence in the optimization results.

The above shortcomings of MOEAs lead many researchers to turn to scenario analysis methods for an optimal USWM system design (Cano and Barkdoll *2017*), especially for robust decision making under uncertain conditions (Urich and Rauch, *2014*; Zischg et al., *2017*). Compared to MOEAs, which are objective driven methods, scenario analysis methods are driven by a set of influencing factors. That is, each planning scenario is often designed on the basis of certain prerequisites. For example, Dong et al. (*2017*) designed three system configurations with green roofs, permeable pavement and storage tanks from the perspective of flooding, environmental and technical severity, and compared their resilience to future rainfall extremes and urban land use change. Similarly, Casal-Campos et al. (*2015*) studied more planning scenarios by integrating a regret-based approach. However, the reliability of the scenario analysis results is highly dependent on the quality of scenario assumption (Urich and Rauch, *2014*; Zischg et al., *2017*). Moreover, scenario analysis methods give up seeking the most cost-effective planning schemes and often result in solutions far from Pareto optimality (Roach et al., *2016*; Xu et al., *2017*) because identifying the performance of many potential scenarios through exhaustive attack is impossible (Liu et al., *2016a*).

Moreover, LID layout planning within the entire planning area to achieve a given control target is a gradual (i.e., with several stage goals) rather than a single-stage process (Zischg et al., *2017*). However, many of the aforementioned studies (Oraei Zare et al., *2012*; Casal-Campos et al. *2015*; Liu et al., *2016a*; Cano and Barkdoll *2017*; Dong et al., *2017*; Xu et al., *2017*) just drew a final-stage blueprint and did not point out the pathway to realization. Besides, when the control target becomes stricter (e.g., increase NPS pollution removal rate from 50% to 70%) in the future, the traditional MOEAs or scenario analysis methods do not have a proper answer where to place additional LID practices to achieve the new control target, based on the previously implemented LID layout, which may have lock-in effects (Haasnoot et al., *2013*). In summary, the performance deficits during LID implementation cannot be disregarded and Pareto optimality should be guaranteed always (Creaco et al. *2013*). That is, an optimal pathway of multi-stage planning should be established by solving the LID layout optimization problem instead of just throwing out a single-stage static planning scheme.

Inspired by Liu et al. (*2016a*) and Mao et al. (*2017*) who pointed out that cost effectiveness (i.e., average cost per unit control target achieved) determines the favorability of LID practice, this study proposes a new optimization method based on the economic law of increasing marginal costs (MCs) (Fisher, *1961*) and rational choice theory (Blume and Easley *2008*), namely, Marginal-Cost-based Greedy Strategy (MCGS) for LID layout planning. This method takes the essence and discards the weaknesses of MOEAs and scenario analysis methods, and can generate a more reliable performance trade-off with markedly low computational costs. No peer-reviewed literature that applies a greedy strategy to plan an USWM system optimally has yet been found. Moreover, the MCGS process of generating the optimal planning schemes exactly blazes an optimal pathway of multi-stage LID layout planning.

MCGS is applied to the following three case studies in China to verify the above statements using the popular NSGA-II for comparison:

- Case I: independent HRUs and a simple objective;
- Case II: independent HRUs and a complicated objective;
- Case III: dependent HRUs and a complicated objective.

2. Material and methods

2.1. Definition of a MOP

Before introducing the development of MCGS, a general LID layout optimization problem is described, which comprises contradictory objective functions and decision variables.

The first objective function is often related to the environmental goal or control target of an USWM system, such as the reduction in urban runoff volume, peak flow, or NPS pollution discharge. A complicated function form is also acceptable, such as expectation or norm, when future uncertainties or multiple control targets must be considered. The second objective function represents an economic indicator, which can include construction costs, life-cycle maintenance costs, opportunity costs, and socio-economic returns (Liu et al., *2016a*; Cano and Barkdoll *2017*). For illustrative purpose in this methodology study, this study adopts the former two and a discounted cash flow model to calculate the second objective, as expressed in Eq. (1), where C_{cst} is the construction cost of a LID practice, C_{mtn} is the maintenance cost, T is the operational life span, and R is the annual discount rate. This form of economic indicator has been used by many researchers (Liu et al., *2016a*; Roach et al., *2016*). Appendix C.1 records detailed information about the price information of LID practices in Chinese pilot Sponge Cities.

$$C_{tot} = C_{cst} + C_{mtn}\sum_{t=1}^{T}\frac{1}{(1+R)^t} \tag{1}$$

A HRU can either be a subcatchment or a group of parcels with the same land use type and hydrologic characteristics. A decision variable is the percentage of a certain underlying surface with a LID practice implemented in a HRU (referred to as "placing ratio" hereinafter). For example, the LID layout shown in Fig. 1 has two decision variables, namely, the placing ratio of porous pavement in an impervious road or square (φ_1) and the placing ratio of bioretention in green space (φ_2). The value range of a decision variable is often from zero to one, unless additional constraints, such as fire lane reservation, must be considered. If a certain LID practice is unsuitable for a HRU, then its placing ratio will be fixed at zero and will not participate in the optimization process. According to the above definition, the total amount of decision variables within the entire planning area is the sum of the decision variables in each HRU.

2.2. Development of MCGS

A greedy strategy is an algorithmic paradigm that starts optimization from the status quo and makes a locally optimal decision at each subsequent stage with the hope of finding a series of global optimums (Black *2005*). That is, a greedy strategy continuously chooses the best choice from a finite number of alternatives based on current rather than subsequent situations till all predefined constraints are breached. For LID layout optimization, all the decision variables are constrained within their upper limits. Given that the starting and ending points are known (the starting point is the status quo without any LID practice implemented, and the ending point is the planning scheme with all the decision variables equal to their upper limits), MCGS therefore aims to seek an optimal path where all the intermediate-stage solutions satisfy Pareto optimality. Inspired by rational choice theory that insist on the minimization of MCs to make locally or globally optimal decisions (Blume and Easley *2008*), the best choice can be defined as the one that achieves the minimum MC. Accordingly, the MCGS flowchart is designed as Fig. 2, which contains an output loop and an inner loop. The output loop aims to achieve the minimization of MCs, while the inner loop aims to accelerate the optimization with the help of the economic law of increasing MCs.

In economics, MC measures the opportunity cost that arises from producing one more unit of a good. Expanded to an USWM system, the marginal cost of placing an extra ratio of a certain LID practice can be defined as:

$$MC_{i,t} = \frac{\mathrm{d}C_i}{\mathrm{d}U}\bigg|_{\boldsymbol{S}_{t-1}} \approx \frac{C_{i,t}-C_{t-1}}{U_{i,t}-U_{t-1}}\bigg|_{\varphi_{i,t}=S_{i,t-1}+\Delta} \tag{2}$$

where i is the index of a decision variable; t is the index of an intermediate stage of LID layout planning; $\boldsymbol{S}_t$ is a vector that represents the placing ratios of each LID practice at the t–th stage; U and C are the environmental and economic indicators of an USWM system, respectively; φ represents the decision variable; and Δ is a constant increment of the placing ratio of any LID practice. The second term is represented

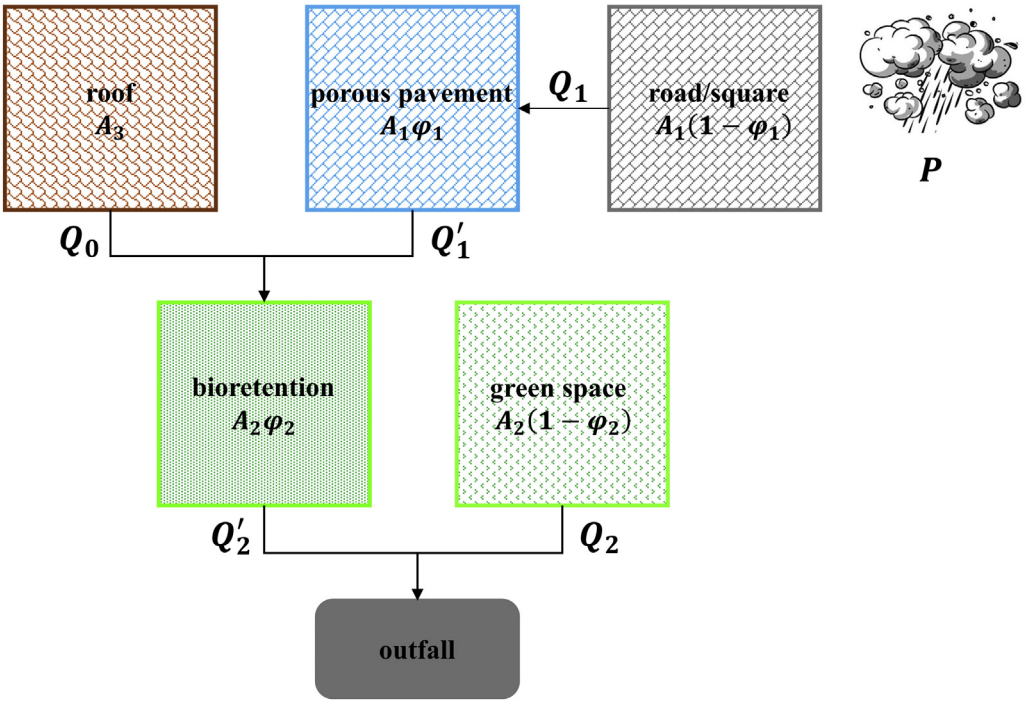

Fig. 1. Conceptual model of implementing LID practices in series in a HRU.

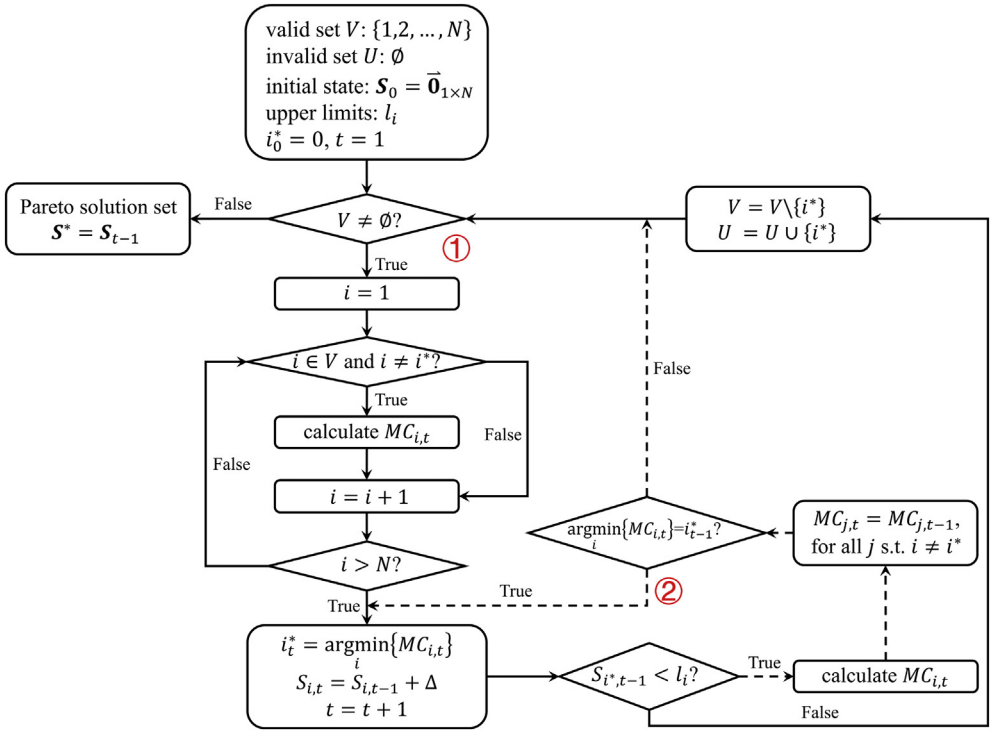

Fig. 2. Programming flowchart of MCGS. Digit One with the solid arrows represents the output loop. Digit Two with the dashed arrows represents the inner loop.

in a derivative form. The third term is represented in differential form, which will be used to estimate MCs in this study. When a LID practice is fully implemented, that is, φ reaches its upper limit, the corresponding MC is assigned to invalid. According to this definition, the economic law of increasing MCs can be expressed by the following two conditions, and is true in the studied USWM systems because of the reasons presented in Appendix B.

$$\frac{\partial MC_i}{\partial \varphi_i} \geq 0 \tag{3}$$

$$\frac{\partial MC_j}{\partial \varphi_i} \geq 0, \forall j \neq i \tag{4}$$

After making an optimal choice (i^*) at a certain stage $t-1$, MCGS firstly enters the inner loop. The inner loop will estimate the MC of choice i^* at the next stage t ($MC_{i^*,t}$) according to Eq. (2). Eqs. (3) and (4) indicate $MC_{i,t} \geq MC_{i,t-1}$ at all times. Thus, if $MC_{i^*,t} < \min_{i \neq i^*}\{MC_{i,t-1}\}$ still holds, then $MC_{i^*,t} < \min_{i \neq i^*}\{MC_{i,t}\}$. That is, practice i^* is still the most cost-effective choice at stage t. Therefore, there is no need to calculate the MCs of the other choices. Otherwise, MCGS exits the inner loop and returns to the output loop. The output loop will estimate the MC of each decision variable that is still below its upper limit (i.e., sufficient place exists for implementing the practice) except choice i^*. The optimal choice corresponds to the one with the minimum $MC_{i,t}$. Once any two adjacent stages favor the same decision variable, the existence of an inner loop can save $N-1$ times of model simulation and reduce the computational budget, where N is the number of decision variables. For other environmental problems where the law of increasing MCs may not be always true, the MCGS user just needs to ignore the inner loop and the output loop still works.

2.3. Case study overview

For all the case studies, the entire planning district should be partitioned first into different HRUs. For illustrative purpose, the LID layout is placed in each HRU of all three cases as shown in Fig. 1. The possible LID practices (i.e., decision variables) and the corresponding constraints are determined by local conditions and a multi-criteria siting system (e.g., SUSTAIN) (Shoemaker et al., *2009*; Jia et al., *2013*).

Cases I and II are conducted in the urban districts of Suzhou City, China. Suzhou is located on the west of Shanghai in the Yangtze River Delta (Fig. 3(a)). The city has a humid subtropical climate. Impacted by the summer monsoon from the Eastern China Sea, most of the precipitation is concentrated from February to October. Recent decades have witnessed the rapid urbanization in Suzhou. Suzhou has been in the list of top ten Chinese cities because of its high urbanization ratio at 75% and economic development, which has caused the city to suffer severe "city syndrome," particularly the eutrophication in Lake Tai (Fig. 3(a)) in recent years.

Cases I and II represent a watershed-scale LID layout optimization by coupling optimization algorithms with a conceptual rainfall-runoff model, namely, the Long-Term Hydrologic Impact Assessment-Low Impact Development (L-THIA-LID) model (Liu et al., *2015b*). Similar to a recent study (Liu et al., *2016a*), independent HRUs are assumed because the rainwater pipe network is often ignored at watershed scale (Fig. 3(c)). Considering that phosphorus is an on-going concern in Suzhou, Cases I and II choose the removal ratio of total phosphorus loads in stormwater runoff as the environmental goal. The first objective functions are expressed as Eqs. (5) and (6). The difference is that Case I conducts optimization under fixed model settings, whereas Case II considers the influence of three sources of future uncertainties, i.e., climate change, urban expansion, and LID performance degradation, on the performance of each LID planning scheme. The basic idea is robust optimization (Deb and Gupta, *2006*) that integrates the weighted average of the expected and worst-case outcomes into the first objective function as recommended by McInerney et al. (*2012*). The L-THIA-LID model characterizes these deep uncertainties as random parameters ($\boldsymbol{\theta}\sim$), making the first objective function relatively complicated (Eq. (6)). For each random parameter, the value range is assumed to be from 0 to 10%. The Latin-Hypercube sampling method (Ye, *1998*) is helpful in generating a broad range of possible future projections for estimating the expectation of the environmental goal.

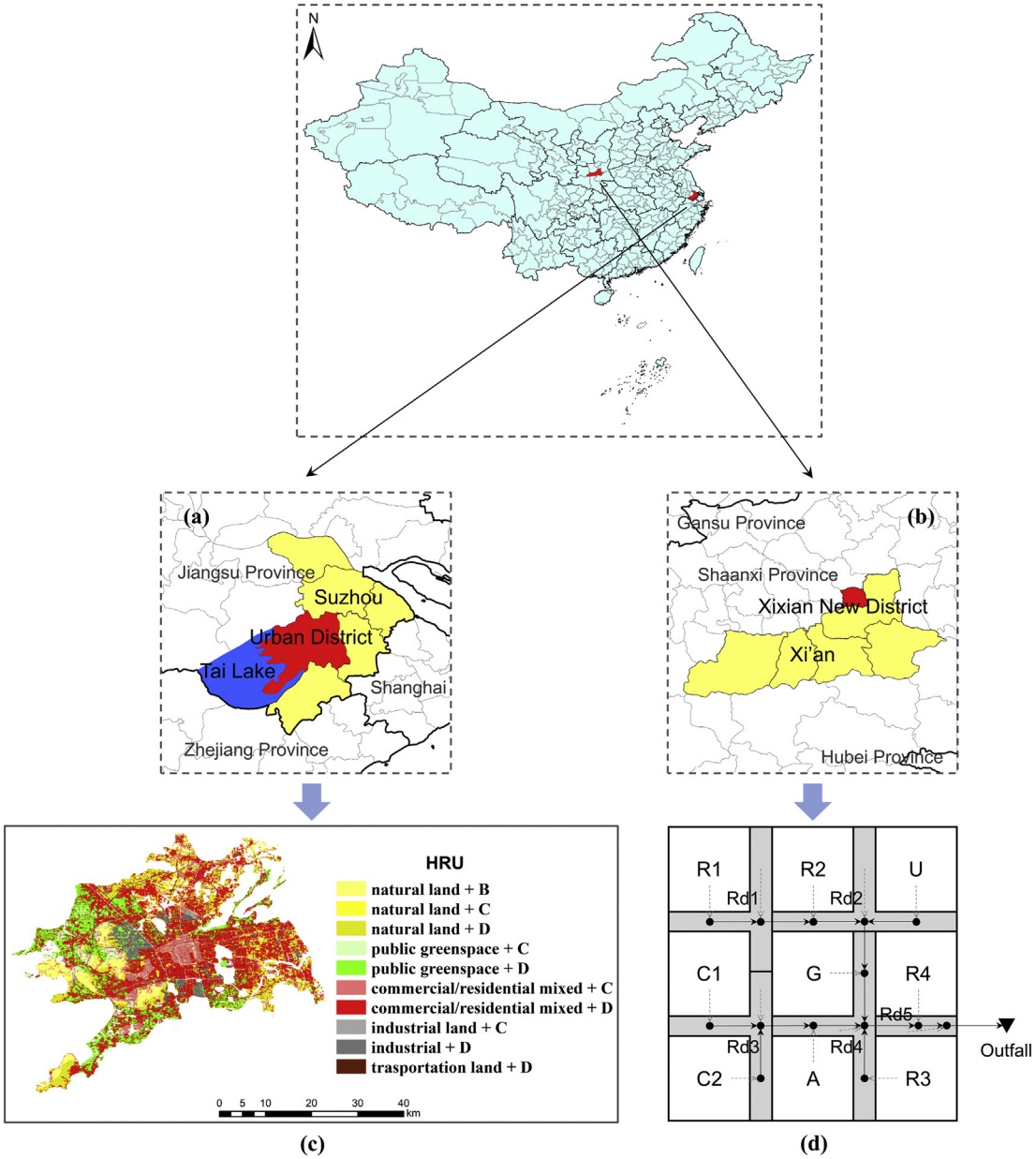

Fig. 3. An overview of study sites. Cases I and II: Suzhou urban district (left); Case III: Xixian New District (right).

A total of 17 decision variables are involved in Cases I and II. The upper limit of each decision variable is designated based on the field conditions (Table C.5). Given that the research purpose is a methodology comparison under the same case study settings rather than to build an accurate model, the tendency of such subjective settings to deviate from real situations is of no consequence. This logic is still established for Case III. The L-THIA-LID model uses the daily precipitation data from 2012 to 2016 (from the end of one La Niña phenomenon to the end of the latest La Niña phenomenon) as the forcing data. Appendix A.1 briefly illustrates the mechanisms of LID simulation in series in the L-THIA-LID model. Appendix C.2 records detailed information about the HRUs and the decision variables, monitoring data, and local parameters in Suzhou urban district. Appendix C.2 also demonstrates the parameterization of the three uncertain factors in Case II.

Case III is conducted in a small community in Xixian New District, China, which is one of the thirty pilot Sponge Cities. Xixian New District is located on the northwest of Xi'an in the Loess Plateau (Fig. 3(b)). Impacted by the loose soil and temperate continental climate, soil erosion in wet seasons (summer) and drought in dry seasons (winter) are the two main environmental concerns of the city. Hence, the first objective function of Case III simultaneously considers runoff capture (for reuse in dry periods), the decrease in total suspended solid (TSS) loads (to alleviate environmental degradation), and the reduction of pipe peak flow (for system safety), as expressed in Eq. (7). Compared with Case I, Eq. (7) is also a substantially complicated form.

Case III represents a block-scale LID layout optimization by coupling optimization algorithms with the calibrated and validated SWMM (Rossman and Huber, *2016*). The community has a traditional drainage system and all HRUs are connected by a rainwater pipe network (Fig. 3 (d)). Thus, the assumption of independent HRUs no longer holds during flooding period because of the limited conveyance capacity of rainwater pipes. For example, implementing additional LID practices in a subcatchment to eliminate ponding in its outlet node will enlarge the available channel-conveyance capacity for an upstream subcatchment and shorten its runoff retention time. Moreover, unlike the L-THIA-LID model, simulation of runoff routing in rainwater pipes makes the relationship between LID placing ratios and drained-out flow highly nonlinear. The above two reasons will make the MC variation trends relatively

complex. A total of 20 decision variables are involved in Case III. SWMM uses a Chicago-approach synthetic rainfall event (Keifer and Chu, *1957*) with a five-year return period as the forcing data. Appendix A.2 briefly introduces the mechanisms of LID simulation in series in SWMM. Appendix C.3 records detailed information about the HRUs and the decision variables, synthetic rainfall event, monitoring data, and the calibrated parameters in Xixian New District.

$$U_1 = 1 - \frac{TP}{TP'} \tag{5}$$

$$U_2 = 1 - \frac{0.5 * \left(\mathrm{E}[TP(\boldsymbol{\theta}\sim)] + \max_s\{TP(\boldsymbol{\theta}_s)\}\right)}{TP'} \tag{6}$$

$$U_3 = 1 - \sqrt{0.6\left(\frac{Runoff}{Runoff'}\right)^2 + 0.3\left(\frac{TSS}{TSS'}\right)^2 + 0.1\left(\frac{Peakflow}{Peakflow'}\right)^2} \tag{7}$$

Where, *variables* are the control targets after implementing LID practices, and *variables′* are the control targets before implementing LID practices under current conditions.

2.4. Configurations of the optimization algorithms

The sole hyper-parameter of MCGS (i.e., Δ) is set as 2.5% for all the decision variables in three case studies.

The extensively used NSGA-II (Deb et al., *2002*) is also applied to generate optimal LID layouts for performance comparison with MCGS, because the high performance and capabilities of NSGA-II in handling MOPs are well documented (Kollat and Reed *2006*; Nicklow et al. *2010*). After several trials to search for a good-quality performance trade-off, this study finally sets the size of the solution sets (i.e., population size, M), the maximum number of iterations (T), the crossover probability (P_1), and the mutation probability (P_2) of NSGA-II to 80, 400, 0.75 and 0.10, respectively. Apart from the maximum number of iterations, a convergence criterion, namely, hypervolume indicator (*HV*) is also defined to decide whether the evolution process should stop. *HV* is expressed as Eq. (8). For NSGA-II, *HV* is the sum of the unreachable (V_u) and potential areas (V_p) (Fig. 4(a)); for MCGS, *HV* is equivalent to V_u (Fig. 4(b)). A *HV* closer to zero means better convergence. NSGA-II will quit the evolution when the improvement of the *HV* within the consecutive five iterations is below 1.0×10^{-6}. Further explanation of the NSGA-II operation can be found in the literature (Deb et al., *2002*).

$$HV = \begin{cases} V_u + V_p & for\ NSGA-II \\ V_u & for\ MCGS \end{cases} \tag{8}$$

NSGA-II is extracted from SUSTAIN (Shoemaker et al., *2009*). MCGS and NSGA-II are encoded with python 2.7. All three cases with MCGS and NSGA-II are run on the same personal computer with an Intel Core i7-7700 CPU (3.6 GHz) and 16-GB RAM. Only one thread is occupied for each case to compare the computational performances of MCGS and NSGA-II reasonably.

3. Results and discussion

3.1. Performance trade-offs and convergence

The Pareto solution sets of MCGS and NSGA-II in each case study are plotted in Fig. 5(a), (b) and (c), all presenting convex trends. On each trade-off curve, an evident turning point of the curve slopes from steeper to flatter is observed, which are located around $U_1 = 0.6$, $U_2 = 0.5$, and $U_3 = 0.6$, respectively. This means that after this turning point, the total cost would increase more dramatically than before the turning point when the control target is incremented by one more unit. Thus, the convex shape of the trade-off curves conforms to the law of increasing MCs. A detailed discussion of this point is presented in Section 3.2.

The NSGA-II results are markedly close to the MCGS results. However, MCGS yields a better performance trade-off that dominates the NSGA-II results in all three cases with different system settings and control targets. As shown in Fig. 5(a), (b) and (c), many NSGA-II solutions are below the MCGS performance trade-offs, and only a few points are located exactly on the curve. This means that the planning scheme yielded by MCGS costs no more than that by NCGA-II to achieve the same control target. To achieve the environmental goal of the turning points (Jia et al. (*2017*) suggested that the turning-point solution be adopted as the final plan), for example, Cases I, II, and III cost 19.10, 21.58, and 25.62 million CNY per km^2 according to the MCGS results, respectively, and cost 19.81, 22.19, and 27.24 million CNY per km^2 according to the NSGA-II results, respectively. That is, MCGS cost 3.6%, 2.8%, and 5.9% less than NSGA-II.

These significant advantages are eventually reflected by the *HV* gaps. MCGS therefore presents a better convergence given that *HV* acts as a convergence criterion. As shown in Fig. 5(d), MCGS yields significantly smaller *HV*s in all the cases than NSGA-II. In Cases I, II, and III, the *HV* gaps between these two methods are 0.0060, 0.0129, and 0.0243, respectively, which account for 1.47%, 2.77%, and 4.58% of the *HV*s of NSGA-II. As the USWM system becomes more complex (i.e., more decision variables are involved or the control target becomes more complicated), the gap would increase substantially. This situation implies that MCGS presents a more reliable performance than NSGA-II in LID layout optimization, particularly for the optimal planning of a complex USWM

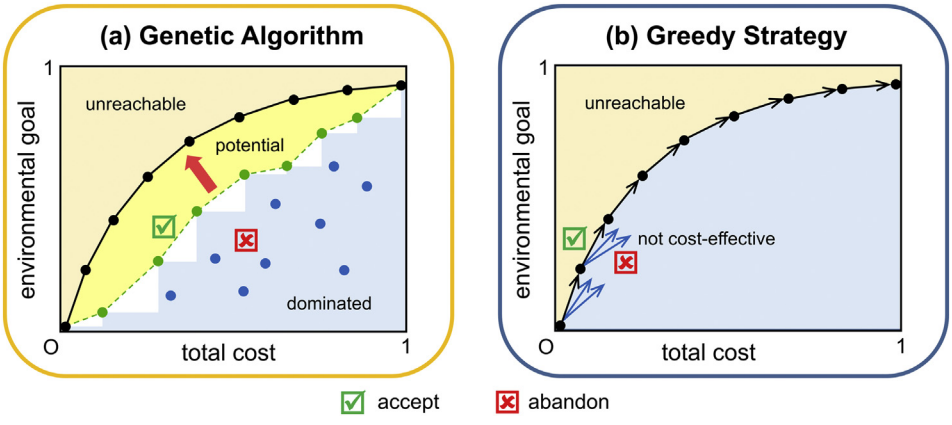

Fig. 4. Graphical explanations and comparisons of NSGA-II (left) and MCGS (right).

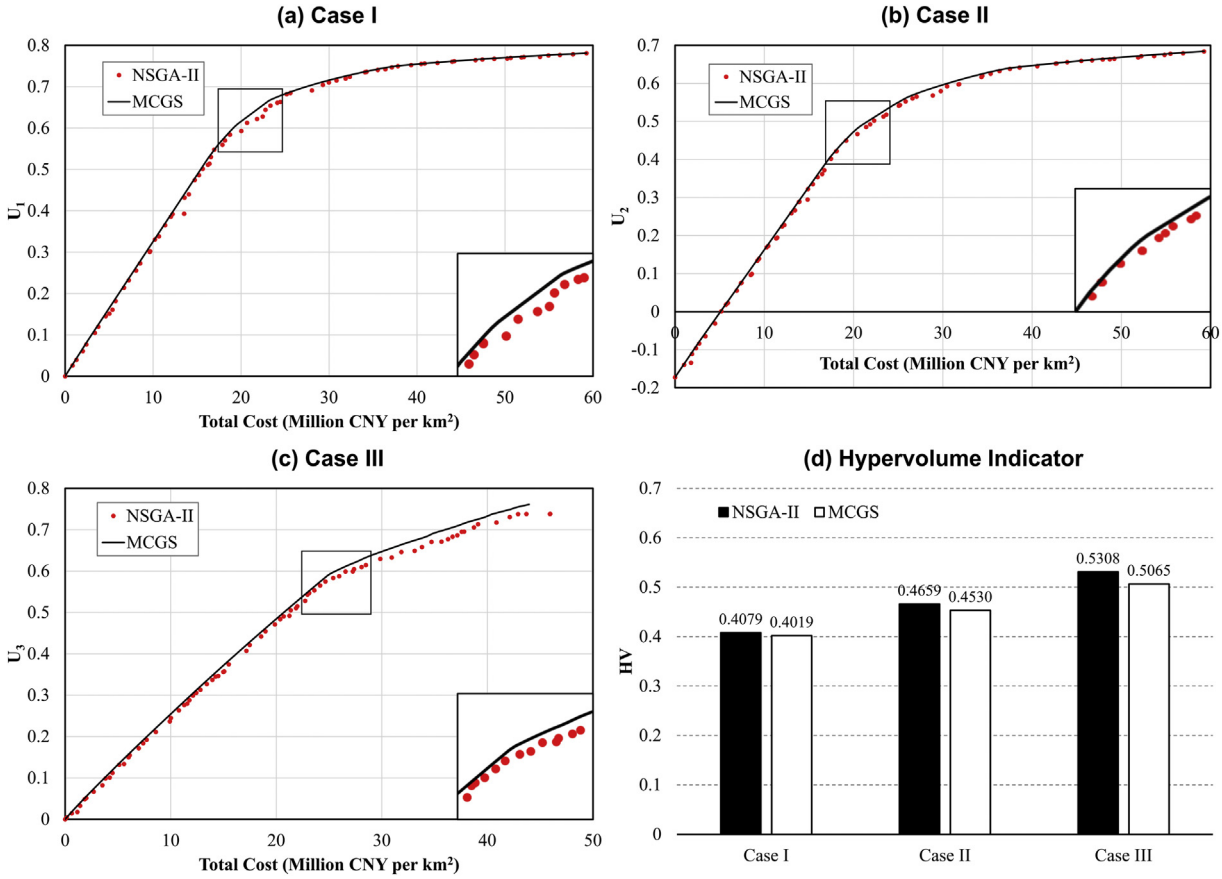

Fig. 5. Comparisons of performance trade-offs and convergence between MCGS and NSGA-II. The turning points in (a), (b), and (c) are zoomed out.

system. Moreover, these gaps can well estimate V_p for NSGA-II according to Eq. (8).

The impact of future uncertainties on optimization results can be reflected by comparing Fig. 5(a) and (b), whose trade-off curves have similar shapes. The trade-off curve of Case I starts from $U_1 = 0$, while Case II starts from a 17.3% performance deficit, implying future system degradation resulting from climate change and urban expansion. Within the definition of U_2, investing about 5 million CNY per km^2 in the optimal LID layout can neutralize these negative impacts and help the city maintain its current hydrologic conditions (Fig. 5(b)). In this sense, this amount of investment can be deemed as "opportunity cost of robustness." The trade-off curve of Case I ends at $U_1 = 0.781$, while Case II ends at $U_2 = 0.684$ with the same amount of investment, implying that the performance deficit has decreased to 9.7%. This result further proves the positive effects of LID on USWM system despite consideration of long-term LID performance degradation in Case II. Future study may focus on quantification of the impact of each individual uncertain factor with the help of global sensitivity analysis (Jia et al., *2018*).

3.2. Detailed Pareto solutions and MC variation trends

The detailed Pareto solutions (the placing ratios of each LID practice, namely, φ_1 and φ_2 in Fig. 1) of MCGS and NSGA-II and the corresponding MC variation trends are plotted in Fig. 6, taking Case I as an illustrative example. The following discussion and conclusions can also be made with respect to Cases II and III.

As shown in the MCGS results (Fig. 6(a)), MC is a non-decreasing function of the control target for each LID practice. This means that MCGS strictly follows the law of increasing MCs, which is one of the methodological foundations. Although the NSGA-II results seem to have irregular patterns (Fig. 6(c)), the law of increasing MCs can still be identified to some extent due to the similar variation trends of the placing ratios and MCs between these two methods. For example, practice pp8 (marked by blue squares) becomes favorable at $U_1 \approx 0.75$ in both the MCGS and NSGA-II results. In addition, for both MCGS and NSGA-II, the MC of pp8 begins increasing after $U_1 \approx 0.08$, flattens after $U_1 \approx 0.56$, and increases again at $U_1 \approx 0.70$.

To further demonstrate the stepwise minimization of MCs, a more specific example is given by three black dashed lines in Fig. 6. Before Line One ($U_1 \approx 0.01$), br14 always has the smallest MC within its value range. MCGS identifies br14 (marked by red circles) as the most cost-effective practice (Fig. 6(a) and (b)). Thus, br14 is the first practice to be selected. Meanwhile, its placing ratio continues to increase until it is 100% implemented. After Line One, br7 (marked by orange circles) becomes the most cost-effective among the residual practices as no place for implementing br14 exists anymore. Thus, br7 becomes favorable until Line Two ($U_1 \approx 0.08$). At this point, places for implementing br7 ($\varphi_2 < 0.50$) still exist. However, br7 has reached its critical percentage ($\varphi_2 \approx 0.375$) when all the upstream runoff can be exactly reduced by br7 and no overflow would occur any more. After this critical percentage, a certain part of br7 capacity would be wasted if its placing ratio continues to increase. Therefore, the MC of br7 increases (a more detailed explanation of the MC variation trend can be found in Appendix B) and jumps over the MC of br8 (marked by green circles), as seen in Fig. 6(a). This means that br7 becomes less favorable than br8 and stops being implemented. A similar logic can explain the variation trends of br7 and br8 between Lines Two and Three ($U_1 \approx 0.52$). Although the three black dashed lines are given by the MCGS logic, the results are coincident that these three lines accurately identify a similar pattern in the NSGA-II results that describe the MC variation trends and the placing ratio changes of br7, br8, and br14 (Fig. 6(c) and (d)).

Intuitively, MCGS and NSGA-II have different mechanisms. That is, the former is based on rational choice theory (the stepwise

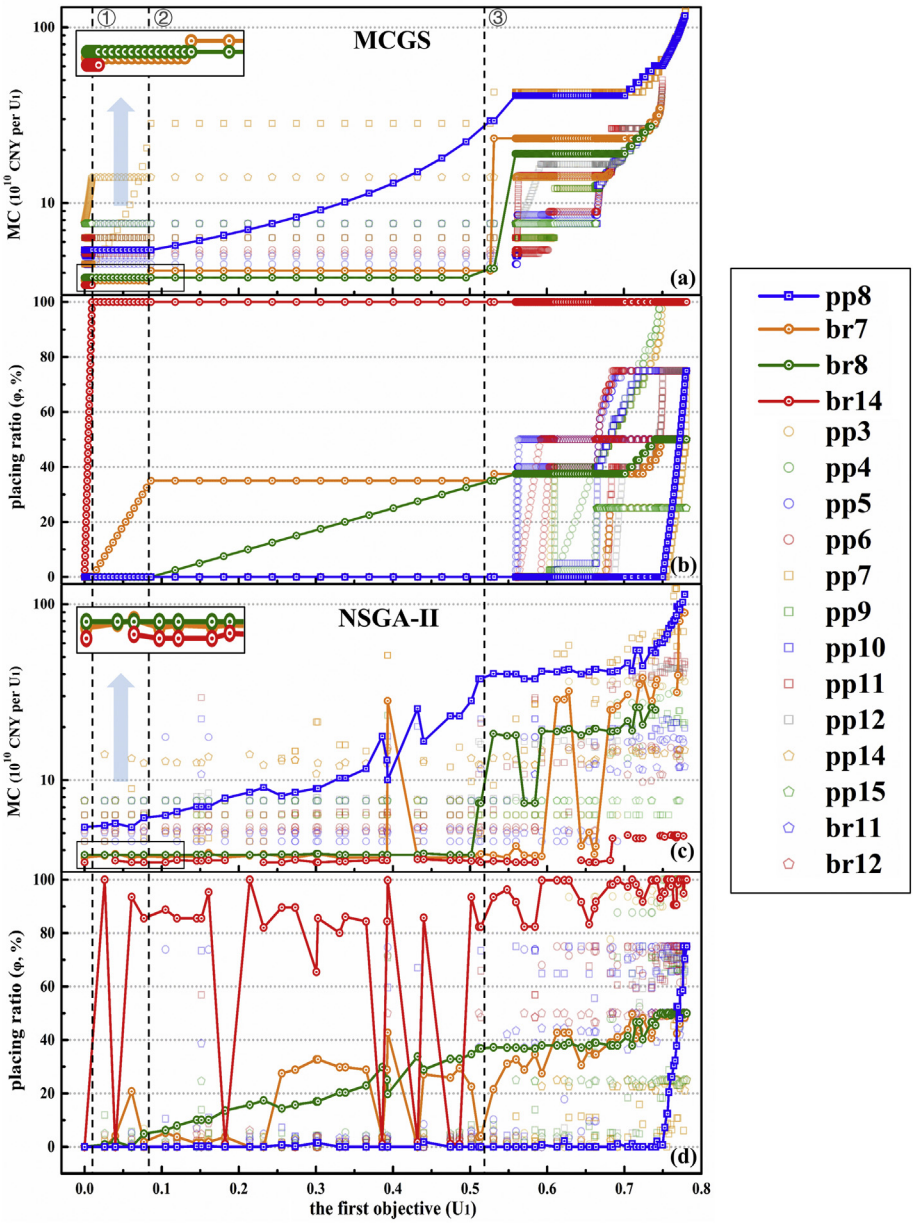

Fig. 6. Detailed Pareto solutions for various percentages of implementing LID practices and the corresponding MC variation trends of Case I.

minimization of MCs), and the latter is based on evolution theory. Nevertheless, the above discussion supports that MC is also a determining factor that drives the NSGA-II process of LID practice selection. The difference is that in NSGA-II, MC functions in an indirect manner, which is subject to the inevitable random factors in NSGA-II (e.g., the crossover and mutation processes). On one hand, the crossover and mutation operators function as an attractive force. They choose the "good genes" (optimal values of decision variables) and discard the bad ones, and consequently push each solution to become more cost-effective. On the other hand, these random factors seem like a repulsive force. Each solution has an extremely small likelihood of evolving to the most cost-effective (i.e., located exactly on the theoretical performance trade-off) because building "better genes" via the crossover and mutation operators is an entirely random event. That is, the convergence of population to the theoretical Pareto optimality within the maximum number of iterations is uncertain. This two-sided characteristic of NSGA-II is a possible reason for the subtle differences between the MCGS and NSGA-II results (e.g., gaps between performance trade-offs).

The major difference is that in the MCGS results, the optimal LID layout that can achieve a high control target contains any optimal solution that achieves a smaller control target, because the former is created based on the latter according to the MCGS mechanisms (Fig. 2). This situation is not true for NSGA-II. For example, in Fig. 6(a) (i.e., the MCGS results), red circles (i.e., valid MCs) only exist before Line One, which corresponds to the 100% placing ratio of br14 at all times after Line One as seen in Fig. 6(b) (according to Section 2.2, there is no need to calculate the MC for a fully implemented practice), whereas in Fig. 6 (c) (i.e., the NSGA-II results), several discontinuous red circles still appear after Line One, and the placing ratios of br14 at these points are all below 100% (Fig. 6(d)). Thus, in the NSGA-II results, the optimal LID layout that can achieve a high control target does not necessarily contain all the optimal solutions that achieve smaller control targets.

That means a certain optimal LID layout that can achieve a small control target may not be adequate for a middle stage to meet a higher control target by further implementing additional LID practices.

Hence, from the perspective of multi-stage LID layout planning, the MCGS results establish an optimal pathway that implementing LID practices along the performance trade-off guarantees Pareto optimality always before reaching the predefined control target. Fig. 7 plots this optimal planning route by projecting the detailed Pareto solutions (Fig. 6(b)) onto the Suzhou map (Fig. 3(c)). The recommended LID construction should start at the traffic land by implementing bioretention (Fig. 7(a)) because the traffic land has a highest ratio of the drained impervious area (Table C.5) and is severely burdened with NPS pollution (Table C.4) resulting from high-intensity human activities. In addition, as shown in Fig. 7(b), a porous pavement is not recommended to be constructed until approximately 55% of the TP loads can be removed by bioretention from stormwater runoff ($U_1 \approx 0.55$). This is because bioretention is much more competitive than a porous pavement in reducing TP loads according to Appendix C.2, despite the slightly higher unit cost (Table C.1). According to Fig. 7, if the local government plans to raise the NPS TP removal rate from 55% to 75% in the future, for example, the city planners just need to place a large area of porous pavement and further increase the bioretention implementation intensity. However, NSGA-II is inadequate for this task. If the city plans to implement additional LID practices based on the existing projects to achieve a higher control target, part of the constructed LID practices should be removed to maintain cost effectiveness according to the NSGA-II results, which is impractical.

3.3. Computational performance

MCGS often obtains a larger solution set than NSGA-II (Table 1), which provides city planners with more choices for selecting a final planning scheme. For NSGA-II, the solution set size is directly designated by setting M. As mentioned in Section 2.4, M = 80 is the result of searching for a good-quality performance trade-off. For MCGS, the solution set size depends on the choice of Δ and can only be known after the optimization process ends. For an MOP with over ten decision variables and Δ ≤ 0.05, the final solution set size is often larger than 100. However, because of the same fixed Δ used for different decision variables for different iteration loops, the distance of the control targets between the two adjacent solutions are often not uniform. As seen in Fig. 6(b), the solutions between Lines Two and Three ($0.08 < U_1 < 0.50$) are much sparser than those in other zones, and even sparser than the same zone in the NSGA-II results Fig. 6(d). Fortunately, as mentioned before, a solution with a lower control target is a subset of any solution with a higher control target in the MCGS results. Thus, a proper interpolation in the sparse zone may help it become denser. In addition, introducing a self-adaptive adjustment of Δ is an important direction for further improvement of MCGS.

Table 1
Comparison of solution set sizes of MCGS and NSGA-II.

Optimization algorithm	Solution set size		
	Case I	Case II	Case III
NSGA-II	80	80	80
MCGS	461	461	245

Computational efficiency is measured by CPU usage and model running times. According to Table 2, as for the entire optimization process, NSGA-II CPU time is nearly 8–49 times as much as that of MCGS, and the model run times are nearly 10–56 times more than that of MCGS. On average, NSGA-II CPU time is nearly 26–276 times as much as MCGS, and the model run times are nearly 31–325 times more than that of MCGS to obtain one optimal solution.

In Cases I and II, MCGS take only 1.23 and 1.75 model run times (7.2% and 10.3% of the total amount of decision variables) to obtain one optimal solution, respectively, while in Case III, this task costs 12.5 model run times (62.5% of the total amount of decision variables) (Table 2). This indicated that in Cases I and II, MCGS runs mainly on the inner loop, whereas in Case III, MCGS runs mainly on the output loop. As is explained in Section 2.3, the main reason lies in the involvement of a rainwater pipe network in Case III. At the beginning of the optimization, the existing flooding nodes make the MC variation trends relatively complex and Eqs. (3) and (4) scarcely take equal signs (Fig. D.1). However, in Cases I and II, Eqs. (3) and (4) take equal signs at many steps at the beginning of the MCGS process (Fig. 6(a) and Fig. D.1), which provides favorable conditions for MCGS to maintain in the inner loop.

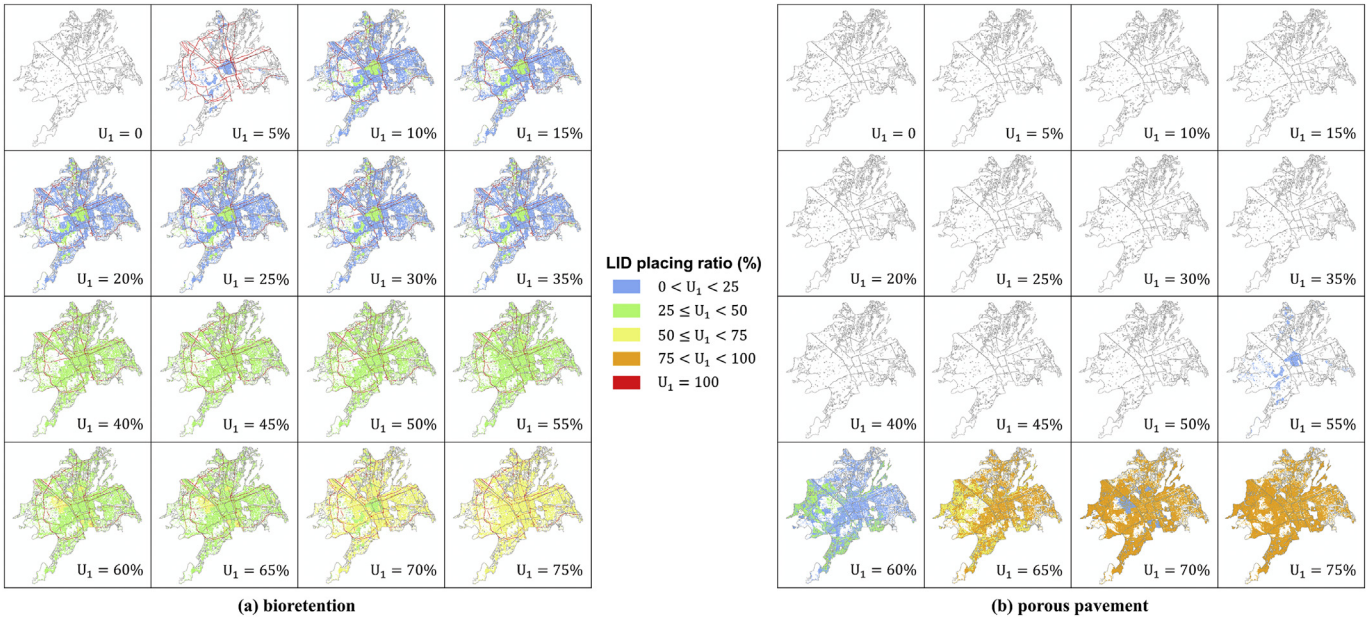

Fig. 7. Optimal route of multi-stage LID layout planning in Case I.

Table 2
Comparison of the computational efficiencies of MCGS and NSGA-II.

Optimization algorithm	CPU time (s)			Model run times		
	Case I	Case II	Case III	Case I	Case II	Case III
NSGA-II	3462.473 (43.281)[a]	92,721.756 (1159.022)	54,217.368 (677.717)	32,080 (401)	32,080 (401)	32,080 (401)
MCGS	70.647 (0.153)	2358.808 (5.117)	6475.845 (26.432)	566 (1.228)	806 (1.748)	3063 (12.502)

[a] Numbers in the brackets mean average computational efficiency for each optimal solution.

Considering that in Case III, MCGS is 8.37 times faster than NSGA-II to finish computing, it can be speculated that MCGS can still be several times (perhaps five or six) faster than NSGA-II, if only the output loop is occupied during the entire optimization process.

In all three case studies, NSGA-II quit the evolution process because of reaching the maximum number of iterations rather than meeting the convergence criteria. As seen in Table 2, NSGA-II has run a total of 401 generations, which is equal to the predefined T plus the one used for creating an initial population. If the city planner wants to continue improving *HV* until the convergence criteria is satisfied, a considerable amount of extra computational resources is necessary. Even worse, whether NSGA-II convergence can be achieved within a finite number of iterations is also uncertain for LID layout optimization problems.

Apart from the great advantages in time complexity, MCGS is also superior to NSGA-II in space complexity (i.e., RAM usage, Table 3). These two methods need to temporally remember the output of the latest iteration. MCGS first calculates the MC of each solution in the latest generation and carries forward the one with the minimum MC to produce the next generation, whereas NSGA-II uses the latest generation as the parent for producing the next generation with the same size. According to these mechanisms, the number of solutions that MCGS must remember at a time is no more than the total amount of decision variables (Fig. 2), whereas that of NSGA-II is twice as large as population size (M) (Deb et al., *2002*). To maintain gene diversity during optimization, M is usually several times larger than the amount of decision variables. Therefore, the RAM usage of MCGS must be smaller than that of NSGA-II.

4. Conclusions

Cost effectiveness is a major concern when implementing LID practices for urban flooding and NPS pollution control. An efficient and more reliable method, MCGS, is developed for LID layout optimization in this study. Compared with the extensively used but elusive NSGA-II, the simple MCGS has the following prominent advantages:

- The success of MCGS in all three case studies with different system settings and control targets indicates that the MC of a LID practice determines its favorability in an USWM system, which provides an intuitive "white-box" mechanism for city planners to learn the optimization process of designing a cost-effective planning scheme;
- MCGS yields a performance trade-off with better convergence and provides more choices for city planners;
- MCGS establishes an optimal pathway for multi-stage LID layout planning; that is, the LID layout planning horizon should be scheduled along the trade-off curve;
- MCGS requires CPU and RAM usages over thirty and seven times less than NSGA-II for obtaining one optimal planning scheme, respectively;
- MCGS has only one hyper-parameter (Δ) that must be carefully selected, whereas multiple trials are necessary for NSGA-II to find an acceptable group of hyper-parameters (M, T, P_1, P_2) and a proper convergence criterion (*HV*) in independent cases.

Table 3
Comparison of the RAM usages of MCGS and NSGA-II.

Optimization algorithm	Solutions in memory		
	Case I	Case II	Case III
NSGA-II	160	160	160
MCGS	17	20	20

Questioning voices at MCGS may come from its model-dependent features. The economic law of increasing MCs (Eqs. (3) and (4)) is one of the methodological foundations of MCGS. These two conditions are not always satisfied in many other environmental systems. Particularly for the second condition, advance in one factor may promote the performance of other factors, and thus reduce the MC. However, breaking the law of increasing MCs only nullifies the inner loop (Fig. 2). The output loop, which is based on rational choice theory, still works. According to the discussion in Section 3.3, MCGS can still yield a reliable trade-off faster than NSGA-II, if the inner loop is inaccessible.

The intrinsic shortcoming of MCGS is that a greedy strategy does not in general produce an optimal path in many optimization problems, unless the problem has the potential to be converted to a Matroid (Bang-Jensen et al. *2004*), which is difficult to prove for any complex environmental system. In this study, MCGS is intended for LID layout optimization in an USWM system, unlike NGSA-II that has been proven effective for many other environmental issues. Fortunately, MCGS performs better than NSGA-II in seeking a cost-effective LID layout with different USWM system settings and control targets. Whether MCGS is suitable for other environmental issues requires further exploration.

Acknowledgement

The authors thank Purdue University for providing adequate computing resources. Also, this research was supported by the National Water Pollution Control Special Project No. 2017ZX07205003, and Tsinghua Fudaoyuan Research Fund (Summer, 2017).

Appendix A. Supplementary data

Supplementary data to this article can be found online at https://doi.org/10.1016/j.scitotenv.2018.05.358.

References

Askarizadeh, A., Rippy, M.A., Fletcher, T.D., et al., 2015. From rain tanks to catchments: use of low-impact development to address hydrologic symptoms of the urban stream syndrome. Environ. Sci. Technol. 49, 11264–11280.
Bang-Jensen, J., Gutin, G., Yeo, A., 2004. When the greedy algorithm fails. Discret. Optim. 1, 121–127.
Bark, S., Choi, D., Jung, J., Lee, H., Lee, H., Yoon, K., Cho, K.H., 2015. Optimizing low impact development (LID) for stormwater runoff treatment in urban area, Korea: experimental and modeling approach. Water Res. 86, 122–131.
Black, P.E., 2005. Greedy algorithm. In: U.S. National Institute of Standards and Technology (NIST) (Ed.), Dictionary of Algorithms and Data Structures.
Blume, L.E., Easley, D., 2008. Rationality. The New Palgrave Dictionary of Economics, 2nd edition Palgrave Macmillan.
Cano, O.M., Barkdoll, B.D., 2017. Multiobjective, socioeconomic, boundary-emanating, nearest distance algorithm for stormwater low-impact BMP selection and placement. J. Water Resour. Plan. Manag. 143 (1), 05016013.
Casal-Campos, A., Fu, G., Butler, D., Moore, A., 2015. An integrated environmental assessment of green and gray infrastructure strategies for robust decision making. Environ. Sci. Technol. 49, 8307–8314.
Cibin, R., Chaubey, I., 2015. A computationally efficient approach for watershed scale spatial optimization. Environ. Model. Softw. 66, 1–11.
Clausen, J., Bedan, E., 2009. Stormwater runoff quality and quantity from a traditional and low impact development. J. Am. Water Resour. Assoc. 45 (4), 998–1008.
Creaco, E., Franchini, M., Walski, T., 2013. Accounting for phasing of construction within the design of water distribution networks. J. Water Resour. Plan. Manag. 140 (5), 598–606.
Deb, K., Pratap, A., Agarwal, S., Meyarivan, T., 2002. A fast and elitist multiobjective genetic algorithm: NSGA-II. IEEE Trans. Evol. Comput. 6 (2), 182–197.
Deb, K., Gupta, H., 2006. Introducing robustness in multi-objective optimization. Evol. Comput. 14 (4), 463–494.

Dong, X., Guo, H., Zeng, S., 2017. Enhancing future resilience in urban drainage system: Green versus grey infrastructure. Water Res. 124, 280–289.
Ferguson, B.C., Frantzeskaki, N., Brown, R.R., 2013. A strategic program for transitioning to a Water Sensitive City. Landsc. Urban Plan. 117 (9), 32–45.
Fisher, F.M., 1961. The stability of the Cournot Oligopoly solution: the effects of speeds of adjustment and increasing marginal costs. Rev. Econ. Stud. 28 (2), 125–135.
Fletcher, T.D., Shuster, W., Hunt, W.F., et al., 2014. SUDS, LID, BMPs, WSUD and more – the evolution and application of terminology surrounding urban drainage. Urban Water J. 12 (7), 525–542.
Gaines, J.M., 2016. Water potential. Nature 531, S54–S55.
Haasnoot, M., Kwakkel, J.H., Walker, W.E., Maat, J.T., 2013. Dynamic adaptive policy pathways: a method for crafting robust decisions for a deeply uncertain world. Glob. Environ. Chang. 23 (2), 485–498.
He, C., Zhao, Y., Huang, Q., Zhang, Q., Zhang, D., 2015. Alternative future analysis for assessing the potential impact of climate change on urban landscape dynamics. Sci. Total Environ. 532, 48–60.
Jia, H., Yao, H., Tang, Y., Yu, S.L., Zhen, J.X., Lu, Y., 2013. Development of a multi-criteria index ranking system for urban runoff best management practices (BMPs) selection. Environ. Monit. Assess. 185, 7915–7933.
Jia, H., Yao, H., Tang, Y., Yu, S.L., Field, R., Tafuri, A.N., 2015. LID-BMP planning for urban runoff control and the case study in China. J. Environ. Manag. 149, 65–76.
Jia, H., Wang, Z., Zhen, X., Clar, M., Yu, S.L., 2017. China's Sponge City construction: a discussion on technical approaches. Front. Environ. Sci. Eng. 11 (4) (18).
Jia, H., Xu, T., Liang, S., Zhao, P., Xu, C., 2018. Bayesian framework of parameter sensitivity, uncertainty, and identifiability analysis in complex water quality models. Environ. Model. Softw. 104, 13–26.
Keifer, C.J., Chu, H.H., 1957. Synthetic storm pattern for drainage design. J. Hydraul. Div. 83, 1–25.
Kollat, J.B., Reed, P.M., 2006. Comparing state-of-the-art evolutionary multi-objective algorithms for long-term groundwater monitoring design. Adv. Water Resour. 29 (6), 792–807.
Larsen, T.A., Hoffmann, S., Luthi, C., Truffer, B., Maurer, M., 2016. Emerging solutions to the water challenges of an urbanizing world. Science 352 (6288), 928–933.
Lee, J.G., Selvakumar, A., Alvi, K., Riverson Jr., J., Zhen, J.X., Shoemaker, L., Lai, F., 2012. A watershed-scale design optimization model for stormwater best management practices. Environ. Model. Softw. 37, 6–18.
Liu, Y., Bralts, V.F., Engel, B.A., 2015a. Evaluating the effectiveness of management practices on hydrology and water quality at watershed scale with a rainfall-runoff model. Sci. Total Environ. 511, 298–308.
Liu, Y., Ahiablame, L.M., Bralts, V.F., Engel, B.A., 2015b. Enhancing a rainfall-runoff model to assess the impacts of BMPs and LID practices on storm runoff. J. Environ. Manag. 147, 12–23.
Liu, Y., Cibin, R., Bralts, V.F., Chaubey, I., Bowling, L.C., Engel, B.A., 2016a. Optimal selection and placement of BMPs and LID practices with a rainfall-runoff model. Environ. Model. Softw. 80, 281–296.
Liu, Y., Theller, L.O., Pijanowski, B.C., Engel, B.A., 2016b. Optimal selection and placement of green infrastructure to reduce impacts of land use change and climate change on hydrology and water quality: An application to the Trail Creek Watershed, Indiana. Sci. Total Environ. 553, 149–163.
Mao, X., Jia, H., Yu, S.L., 2017. Assessing the ecological benefits of aggregate LID-BMP through modelling. Ecol. Model. 353, 139–149.
McInerney, D., Lempert, R., Keller, K., 2012. What are robust strategies in the face of uncertain climate threshold responses? Clim. Chang. 112 (3–4), 547–568.
Marlow, D.R., Moglia, M., Cook, S., Beale, D.J., 2013. Towards sustainable urban water management: A critical reassessment. Water Res. 47 (20), 7150–7161.
Meerow, S., Newell, J.P., 2017. Spatial planning for multifunctional green infrastructure: growing resilience in Detroit. Landsc. Urban Plan. 159, 62–75.
Nicklow, J., Reed, P., Savic, D., et al., 2010. State of the art for genetic algorithms and beyond in water resources planning and management. J. Water Resour. Plan. Manag. 136 (4), 412–432.
Oraei Zare, S., Saghafian, B., Shamsai, A., 2012. Multi-objective optimization for combined quality-quantity urban runoff control. Hydrol. Earth Syst. Sci. 16 (12), 4531–4542.
Prince George's County, Department of Environmental Resources, 1999. Low-impact Development Design Strategies: An Integrated Design Approach. Department of Environmental Resources, Programs and Planning Division.
Roach, T., Kapelan, Z., Ledbetter, R., Ledbetter, M., 2016. Comparison of robust optimization and info-gap methods for water resource management under deep uncertainty. J. Water Resour. Plan. Manag. 142 (9), 04016028.
Rossman, L.A., Huber, W.C., 2016. Storm Water Management Model Reference Manual. U.S. Environmental Protection Agency.
Shoemaker, L., Riverson Jr., J., Alvi, K., Zhen, J.X., Paul, S., Rafi, T., 2009. SUSTAIN – A Framework for Placement of Best Management Practices in Urban Watersheds to Protect Water Quality. Fairfax, VA.
Urich, C., Rauch, W., 2014. Exploring critical pathways for urban water management to identify robust strategies under deep uncertainties. Water Res. 66, 374–389.
USEPA (US Environmental Protection Agency), 2008. Reducing stormwater costs through low impact development (LID) strategies and practices. EPA 841-F-07e006. Nonpoint Source Control Branch, Washington, D.C.
Versini, P.A., Kotelnikova, N., Poulhes, A., Tchiguirinskaia, I., Schertzer, D., Leurent, F., 2018. A distributed modelling approach to assess the use of blue and green infrastructures to fulfil stormwater management requirements. Landsc. Urban Plan. 173, 60–63.
Wang, Y., Sun, M., Song, B., 2017. Public perceptions of and willingness to pay for Sponge City initiatives in China. Resour. Conserv. Recycl. 122, 11–20.
Wang, M., Zhang, D.Q., Su, J., Dong, J.W., Tan, S.K., 2018. Assessing hydrological effects and performance of low impact development practices based on future scenarios modeling. J. Clean. Prod. 179, 12–23.
Xu, T., Jia, H., Wang, Z., Mao, X., Xu, C., 2017. SWMM-based methodology for block-scale LID-BMP planning based on site-scale multi-objective optimization: a case study in Tianjin. Front. Environ. Sci. Eng. 11 (4), 1–10.
Ye, K.Q., 1998. Orthogonal column Latin hypercubes and their application in computer experiments. J. Am. Stat. Assoc. 93 (444), 1430–1439.
Zischg, J., Goncalves, M., Bacchin, T.K., Leonhardt, G., Viklander, M., van Timmeren, A., Rauch, W., Sitzenfei, R., 2017. Info-gap robustness pathway method for transitioning of urban drainage systems under deep uncertainties. Water Sci. Technol. 76 (5), 1272–1281.